International Journal of Hydrogen Energy 153 (2025) 150217

Contents lists available at ScienceDirect

International Journal of Hydrogen Energy

journal homepage: www.elsevier.com/locate/he

Enhanced ammonia decomposition in a structured membrane reactor using a Ru-coated SiC open-cell foam and a Pd-based membrane

Jon Zuniga [a,b], Gaetano Anello [a], Jorge J. Aragón [b], María del Mar Díaz de Guereñu [b], Alba Arratibel [b], Gabriel Marino [c], Cristina Italiano [c], Antonio Vita [c], Fausto Gallucci [a,*]

[a] Sustainable Energy and Process Technology, Department of Chemical Engineering and Chemistry, Eindhoven University of Technology, De Rondom 70, 5612 AP Eindhoven, the Netherlands
[b] Tecnalia, Energy and Environment Division, Mikeletegi Pasealekua 2, 20009 San Sebastian-Donostia, Spain
[c] CNR-ITAE, Via Salita S. Lucia sopra Contesse N.5, S. Lucia, 98126, Messina, Italy

ARTICLE INFO

Handling Editor: Suleyman I. Allakhverdiev

Keywords:
Open-cell foam
Ru-based catalyst
Ruthenium
Pd-membrane
Palladium
Membrane reactor

ABSTRACT

Ammonia decomposition into nitrogen and hydrogen was carried in a structured membrane reactor in this work. The performance of the structured catalyst and the effect of hydrogen permeation through a Pd-based membrane were evaluated. The structured catalyst is based on a commercial silicon carbide open cell foam (40 PPI). The catalyst (3 wt% Ru/CeO_2) was coated by in situ-solution combustion deposition method with sequential cycles to reach the desired catalyst loading (0.31 g cm^{-3}). TEM, SEM, XRD, TPR analysis and adhesion tests were used to characterize the prepared sample. A double-skinned Pd-based membrane has been prepared depositing a selective layer by electroless plating onto porous asymmetric α-Al_2O_3 support. The results proved a successful integration of structured catalyst and membrane. The beneficial effects of the proposed structured membrane reactor configuration enabled an increase in conversion up to 29 % compared with the structured catalyst system. The reaction system allowed an ammonia conversion of 98.4 % and hydrogen purity of 99.2 % at 450 °C and 4 bar. Furthermore, at fixed flow rate, the structured membrane reactor can achieve comparable conversion at operating temperatures about 55 °C lower than in the case of the structured reactor. Moreover, the proposed configuration enabled a conversion higher than the thermodynamic value at 4 and 5.5 bar at fixed temperature (480 °C) and fixed feed flow rate (62 ml min^{-1}). To the best of our knowledge, this work is the first study combining a structured catalyst and a Pd-based membrane for ammonia decomposition.

1. Introduction

The rapid deployment of fossil fuel reserves, along with the dramatic consequences arising from their indiscriminate utilization and associated CO_2 emissions, have attracted global attention in the last decades [1]. Consequently, the necessity of tackling the adverse effects of climate change, while ensuring the energy supply necessary for human activities, has driven the development of new technologies based on more sustainable energy sources with low emissions. In this scenario, hydrogen (H_2) is considered a promising solution as, on one side, it can be produced through water electrolysis employing renewable energy sources and, on the other side, the only product emitted from its combustion/conversion is water [2]. However, the storage and distribution of hydrogen are key challenges in order to employ this gas as energy vector in the energy transition, due to its low volumetric energy density and high ignition energy [3]. Ammonia (NH_3) is considered an excellent hydrogen carrier due to its hydrogen content of 17.6 wt%, carbon free nature and easier storage and transportation compared to pure hydrogen [4].

Nonetheless, ammonia decomposition into hydrogen and nitrogen (N_2) faces several challenges: it is a mild endothermic and equilibrium-limited reaction, thus requiring relatively high temperatures to achieve sufficiently high single-pass conversions [5]. Furthermore, the catalyst employed can degrade due to sintering at elevated temperatures, reducing the overall efficiency [6]. Different reactor types are used for ammonia decomposition, each with its own challenges. Packed bed reactors (PBR) are commonly uses but suffer from poor heat distribution and catalyst deactivation. Non-thermal plasma (NTP) reactors have been also studied in the last decades, but one major issue related to this technology is the energy efficiency of NTP systems along with their

* Corresponding author.
E-mail address: F.gallucci@tue.nl (F. Gallucci).

https://doi.org/10.1016/j.ijhydene.2025.150217
Received 28 November 2024; Received in revised form 24 June 2025; Accepted 27 June 2025
Available online 3 July 2025

durability and cost [7,8]. Recently, to overcome these issues, packed bed membrane reactors (PBMRs) have emerged as a promising solution for hydrogen recovery from ammonia, allowing simultaneous ammonia decomposition into hydrogen and nitrogen along with high purity hydrogen separation, all within a single device [9,10]. Moreover, the membrane reactor technology allows for lower temperature conversion in accordance with the Le Châtelier's principle, as the selective separation of one of the products through the membrane wall shifts the equilibrium, thus overcoming the thermodynamic constraints.

However, the conventional packed bed reactors (PBRs) are limited by heat and mass transfer phenomena. Mass transfer limitations affect catalyst utilization efficiency and hydrogen diffusion from reaction sites to the membrane surface. Parallelly, heat transfer limitations could inhibit fast heat supply and, as a consequence, hinder the endothermic catalytic ammonia decomposition reaction and the membrane separation performance, as both phenomena are extremely sensitive to temperature. Moreover Additionally, in PBRs, the high cost of noble metal catalysts necessary to maintain excellent catalytic activity constitutes a significant portion of the total materials cost.

All the above mentioned limitations could be addressed by implementing a specialized structured network that can maximize specific surface areas, improve catalysts utilization and heat and mass transfer rates. This approach leads to compact, lightweight reactors with reduced overall manufacturing costs [11–13]. Generally, a proper catalyst design can deeply influence the final catalyst features. For instance, Xu et al. studied twisted surfaces in layered materials to create active regions through coordination field distortions, offering a promising strategy for designing highly efficient electron-donating catalysts [14]. Thus, a catalyst with a specific geometric structure, integrated with a hydrogen selective membrane in a structured membrane reactor (SMR) can represent a promising option to enhance the ammonia decomposition process.

Foam catalysts, and more specifically Open-Cell Foam (OCF) catalysts, are a type of structured catalyst characterized by a highly interconnected, sponge-like structure, hence the characteristic name. This porous chaotic structure, in combination with thermally conductive materials, allows excellent heat and mass transfer [15–17]. The heat transfer coefficient of foam catalysts can be significantly higher than that of conventional packed-bed catalysts, thus enabling optimal thermal management of the reaction [18]. Structured systems are highly effective in enhancing heat and mass transfer rates between gas flow and the channel walls, resulting in a more uniform temperature distribution across the entire reaction volume and improved overall process efficiency [19–21]. Moreover, the use of Pd-based membranes to selectively separate H_2 has been recently discussed in literature, for their effectiveness in selectively separating hydrogen. Pd-based membranes exhibit a unique transport mechanism for H_2 permeation, making them highly suitable for this application [22–24]. For instance, Israni et al. successfully carried ammonia decomposition and hydrogen removal through the addition of conventional top-layer and nanopore Pd-based membranes into a membrane reactor packed with a Ni-based catalyst. The proposed results demonstrate that an increase in NH_3 conversion was possible by removing the produced hydrogen from the reaction environment [25]. Similarly, Nailwal et al. studied ammonia decomposition under various operating conditions in both PBR and single-tube PBMR systems. The authors reported an ammonia conversion of 93 % at 500 °C and 1 bar in the PBMR, whereas the reported conversion in PBR at similar operating conditions is about 80 %, demonstrating the beneficial effect of the Pd-based membrane coupling on ammonia conversion [26].

Thus, the focus of this study is to analyze the performance of a structured OCF-based catalyst, coupled with a Pd-based membrane in a structured membrane reactor, for the ammonia decomposition reaction. A compact and highly efficient reaction system has been developed, offering significant improvements in performance and space efficiency. The structured design enhances transport phenomena, ensuring uniform reactant distribution and minimizing thermal gradients, which are critical for maintaining optimal reaction conditions. Additionally, the membrane enables in situ separation of H_2 as it is produced, shifting the reaction equilibrium towards further ammonia decomposition. The integration of reaction and separation processes improves overall efficiency, reduces energy consumption, facilitates post-reactor purification, and enables compact reactor designs. The Pd-based membrane was fabricated realizing a PdAg-based selective layer, deposited by electroless plating, onto a commercial porous asymmetric α-Al_2O_3 support. Prior to tests with Pd-membrane, the performance of the structured catalyst was evaluated by closing the permeate side, simulating a structured reactor system.

The activity tests were conducted using a Ru-based structured catalyst prepared from a commercial silicon carbide (SiC) OCF. Silicon carbide serves as an effective carrier, providing enhanced heat and mass transfer. SiC is a highly durable material known for its chemical stability, as it is inert and resistant to oxidation, making it suitable for harsh environments. Furthermore, it exhibits high mechanical strength while maintaining a relatively lightweight profile. These features are particularly advantageous for ammonia decomposition [27,28].The carrier was loaded with a 3 wt% Ru/CeO_2 catalyst as active phase, prepared via the In Situ-Solution Combustion Deposition (IS-SCD) method [29,30]. Ruthenium is well-known for its high catalytic activity within ammonia decomposition, especially at relatively low temperatures. Cerium oxide (CeO_2), on the other hand, plays a crucial role as a support material, enhancing the stability and performance of the Ru catalyst due to its excellent oxygen storage capacity and redox properties [31].

The advantages of structured catalysis, including enhanced transport phenomena, uniform flow distribution, and reduced pressure drop, make it highly suitable for ammonia decomposition. Furthermore, ruthenium ensures high conversion rates, while the structured design promotes uniform reactant distribution and minimizes thermal gradients. This synergy is particularly interesting in combination with palladium membranes, where precise reaction control is essential for efficient hydrogen separation and overall process performance. The catalytic system was characterized by.

X-Ray Diffraction (XRD), Temperature Programmed Reduction (TPR), Transmission Electron Microscopy (TEM), Scanning Electron Microscopy (SEM), and adhesion tests. Finally, the improvements within ammonia decomposition performance in a structured membrane reactor were investigated.

2. Materials and methods

2.1. Structured catalysts fabrication

A 40 PPI SiC-based OCF (Lanik s.r.o., Czech Republic) employed as carrier was coated with a 3 wt% Ru/CeO_2 catalyst via IS-SCD technique. This SiC carrier was supplied with appropriate geometric features to host a tubular membrane. The large hole in the middle of the structure allows for membrane installation while the three small holes can be used for either installing thermocouples or for installing vertical supports. The geometrical parameters and the physical properties of the OCF employed in this work are detailed in Table 1. The IS-SCD method, which is based on the Solution Combustion Synthesis (SCS), involves a complex self-sustained chemical process, initiated in a homogeneous solution of precursors. This synthesis method features an exothermic, rapid and self–sustaining chemical reaction, where the combustion reactions provide the required heat. For more comprehensive details on SCS and the deposition procedures, please refer to previous studies [32–36]. Briefly, before use, the OCF employed as carrier was cleaned using a 50 % water/acetone solution for 30 min in an ultrasonic bath at ambient conditions, and then dried for 1 h at 120 °C. Subsequently, the OCF was immersed in a solution obtained dissolving high-purity reagents (Sigma-Aldrich®, Massachusetts, USA) in ultra-pure water. Specifically, cerium (III) nitrate hexahydrate ($Ce(NO_3)_3 \bullet 6H_2O$, 434.22 g

Table 1
Geometrical and physical properties of the OCF structure employed in this study.

SiC-based open-cell foam characteristics		
Pore density	(*ppi*)	40
Support diameter	(mm)	40
Support length	(mm)	100
Hole area	(mm^2)	1.05
Pore diameter	(mm)	1.13
Strut thickness	(mm)	0.35
Face diameter	(mm)	1.48
Thermal conductivity	($W\ m^{-1}\ K^{-1}$)	0.40
Void fraction	(−)	0.85
Bed porosity	(%)	85.5
Surface area	($m^2\ m^{-3}$)	1243
Exposed surface area	(mm^2)	1463
Catalytic loading	($g\ cm^{-3}$)	0.31
Catalytic layer thickness	(μm)	23.8–26.6

mol^{-1}) and ruthenium nitrosyl nitrate ($Ru(NO)(NO_3)_x(OH)_y$, $x + y = 3$, 318.10 g mol^{-1}) were used as precursors of the ruthenium and cerium oxide components, respectively, while urea (CH_4N_2O, 60.06 g mol^{-1}) was employed as fuel. High purity reagent-grade (>99 %) chemicals, supplied by Sigma-Aldrich, were used as received. After drying, the coated OCF was placed in an oven, undergoing the combustion phase, and then, rapidly cooled down to ambient conditions. Multiple cycles were needed to achieve the desired catalyst loading (31.23 g) on the support. In each cycle, IS-SCD starts with the dehydration and thermal decomposition of the homogeneous solution, involving several thermally coupled exothermic reactions. These reactions result in the formation of a uniformly distributed catalytic layer on the SiC-based support, accompanied by the release of a large amount of gases. Calcination of the resulting structured catalysts has been carried out using air at 600 °C for 120 min. Fig. 1 shows the images related to the coated (top) and bare (bottom) SiC foam, while Table 1 summarizes the main geometric characteristics of both the bare and coated foams. A more detailed description of the calculations can be found in previous work, Italiano et al. [37].

2.2. Catalysts characterization

In this study a comprehensive analysis of the prepared catalyst was performed. Various characterization techniques were utilized to determine the structural, morphological, and chemical properties of the catalyst. These techniques include X-ray diffraction (XRD) for phase identification. XRD analysis was conducted on D8 Advance diffractometer (Bruker Corporation, Massachusetts, USA) equipped with Cu Kα radiation (λ = 1.5418 Å, 50 kW, 40 mA). The scan rate was set at 1.5 deg min^{-1}, covering a diffraction angle range of approximately 23–80°. The peaks were assigned using the PCPFWIN database.

The reducibility of the sample was assessed via hydrogen H2 temperature programmed reduction (H_2-TPR), carried out using a ChemiSorb 2750 (Micromeritics®, Georgia, USA) and equipped with a thermal conductivity detector (TCD). After loading the calcined catalyst in the instrument, a 30 Nml min^{-1} flow of a 5 vol% H_2/Ar gas mixture was sent introduced to the sample. while The temperature was then ramped from ambient conditions to 1000 °C employing at a heating rate of 20 °C min^{-1}. Then, Hydrogen consumption was calculated using the H_2-TPR profiles of known amounts of CuO.

Multivolume Pycnometer 1305 (Micromeritics®, Georgia, USA) was employed to measure the true volume and relative densities/porosities of both powders and OCFs. First, the sample chamber is filled with helium, reaching a known value of pressure. Then, the expansion of this amount of gas into a known volume leads to a pressure drop. From the two pressure values showed on the instrument, the sample's volume, density, and porosity can be readily obtained.

Detailed morphological and structural analysis was performed through Transmission Electron Microscopy (TEM) and High Resolution Transmission Electron Microscopy (HR-TEM) imaging. These analysis were conducted using a JEM-F200 microscope (JEOL Ltd., Tokyo) equipped with a field emission gun (FEG) operating at 200 kV with a point resolution of 2.3 Å. The reduced samples were subjected to ultrasonic irradiation in isopropyl alcohol and subsequently dispersed onto holey-carbon copper grids. Scanning Electron Microscopy (SEM) analysis was conducted using a XL-30 FEG scanning electron microscope (Philips N.V., Netherlands) operated at 5–20 kV. The fully automated VHX-7000 digital optical microscope (Keyence, Japan) was used to capture high-resolution images of the coated catalytic layer.

The adhesion and mechanical stability of the coated layer were tested using ultrasonic treatment, carried out with a USC 900D device set to 45 kHz frequency and 130 W power, with the process conducted in a 50 vol% petroleum ether solution. The percentage of weight loss observed during this treatment was used as an indicator of the amount of catalyst that had been deposited onto the surface. This method allowed for an assessment of both the coating's durability and the effectiveness of the catalyst deposition.

2.3. Palladium-based membrane preparation and experimental setup

Parallelly, a double-skinned palladium-based membrane was prepared as previously reported by Arratibel et al. [38] on a tubular porous asymmetric α-Al_2O_3 support (Rauschert Kloster Veilsdorf, Germany) with an outer and inner diameters of 14 and 10 mm, respectively. The pore size at of the outer layer of the support is 100 nm. A PdAg-based selective layer, approximately 4–5 μm-thick, was simultaneously deposited by electroless plating, followed by an annealing treatment at 550 °C for 4 h. The selective layer was then coated with a mesoporous

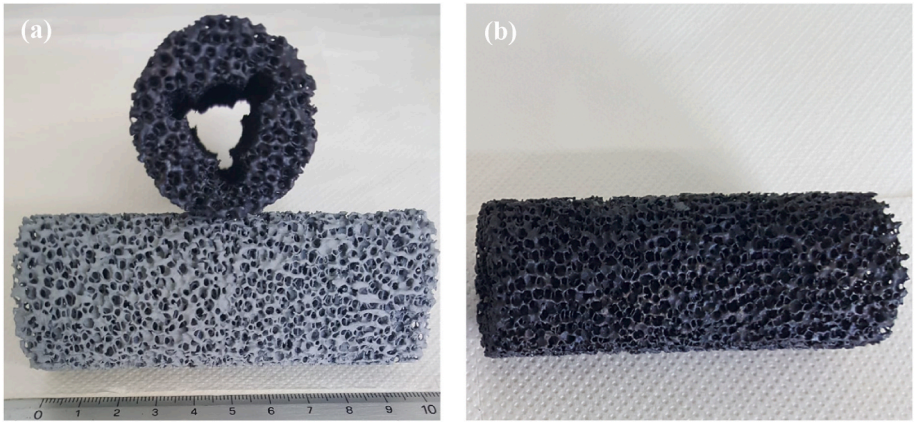

Fig. 1. Images of (a, top) coated and bare (a, bottom) and (b) coated 40 PPI SiC OCF.

YSZ/γ-Al_2O_3 (~1 μm-thick) layer by dip-coating technique and calcined at 550 °C. The double-skinned membrane was sealed with graphite ferrules and connected to the reactor flange that it is reported in the schematic in Fig. 2.

The Ru-based structured catalyst (100 mm long) employed in this work was integrated together with the Pd-based membrane (104 mm long), as shown in Fig. 3.

The catalytic activity tests were conducted feeding pure ammonia into the reactor, where it reacted to produce nitrogen and hydrogen. The latter is able to selectively permeate through the Pd-based membrane. The feed flowrate is controlled by EL-FLOW® mass flow controllers (Bronkhorst®, Netherlands), while the retentate side pressure is managed by an EL-PRESS® pressure controller (Bronkhorst®, Netherlands). The permeate side can operate either at atmospheric pressure or vacuum, while the permeated flow is measured with a mass flow meter (Bronkhorst®, Netherlands). Before determining the composition of both the retentate and permeate streams, the gas flux undergoes a cleaning step. Then, the permeated gases are analyzed with a 990 Micro Gas Chromatograph System (Agilent Technologies Inc., California, USA) equipped with a TCD, while the retentate is analyzed with a 7890A Gas Chromatograph System (Agilent Technologies Inc., California, USA) also equipped with a TCD.

Once the membrane/catalyst assembly is loaded into the reactor, a heating procedure under nitrogen atmosphere takes place, reaching 400 °C with a heating rate of approximately 3 °C min^{-1}. Nitrogen permeation was checked at 4 bar(g) before membrane activation. The Pd-membrane was activated feeding a gas mixture with low oxygen content (5 vol% O_2, 95 vol% N_2) for 2 min. Then, the system is flushed with nitrogen to remove the oxygen present into the reactor. Before starting the experiment with ammonia, hydrogen permeation through the membrane was measured at 400 °C and 1 bar of pressure difference between the retentate and the permeate side. Following the preparation steps, the ammonia decomposition reaction experiments were conducted. These experiments were performed in the temperature range 380–480 °C, in the reaction pressure range 2.6–5.5 bar and for different feed flow rates (62–300 ml min^{-1}). Subsequently, the ammonia conversion (x_{NH_3}) and the H_2 recovery (*HR*) were calculated according to Equations (1) and (2), respectively.

$$x_{NH_3} = \frac{F_{NH_3,in} - F_{NH_3,out}}{F_{NH_3,in}} \quad (1)$$

$$HR = \frac{2\,F_{H_2,permeated}}{3\,F_{NH_3,in}} \quad (2)$$

As benchmark for the structured membrane reactor performance, experimental results for the structured reactor were obtained with the catalyst loaded into the same reactor closing the permeate side under the same reaction conditions.

3. Results and discussion

3.1. Characterization of the catalysts

The results of the detailed characterization of the catalyst are presented in this section. XRD patterns (Fig. 4) indicate the crystal phases of 3 wt% Ru/CeO_2 catalyst deposited on the OCF support. The diffraction patterns of 3 wt% Ru/CeO_2 catalyst collected in the 23–80° (2-theta) range show the typical peaks characteristic of the fluorite structure of ceria corresponding to the (111), (200), (220), (311), (222) and (400) planes (JCPDS no. 34–0394) [39]. The peaks are located at diffraction angles of 28.59°, 33.12°, 47.54°, 56.42°, 59.18° and 69.49°. Weak diffraction peaks related to the RuO_2 phase (JCPDS 21–1172) are also present at diffraction angles of 35.2°, 40.2° and 54.4°. There is a slight shift towards higher angles of the CeO_2 peaks, suggesting the formation of a solid solution (Ru–*O*–Ce) through the partial incorporation of Ru (ionic radius = 0.62 Å) into the cerium oxide matrix (ionic radius = 0.97 Å). The prepared catalyst exhibited ruthenium embedded within the CeO_2 matrix, forming strong interactions between Ru and CeO_2. These

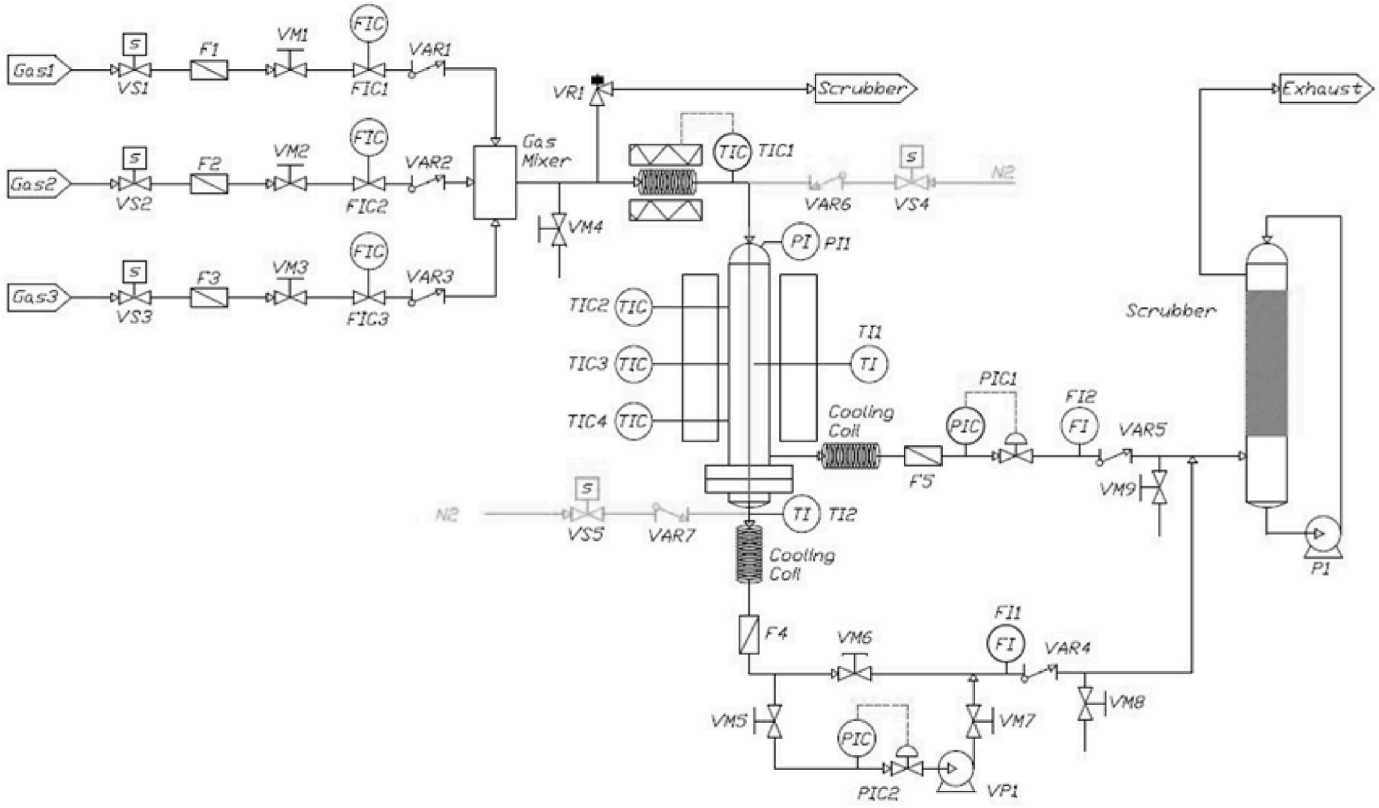

Fig. 2. Schematic of the experimental apparatus used in this work.

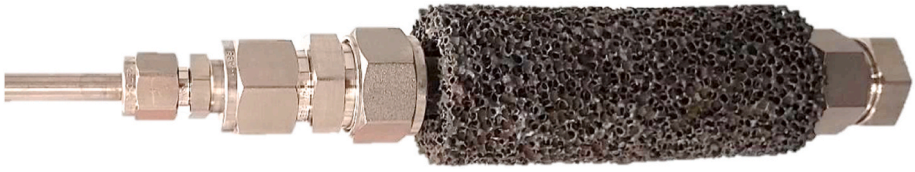

Fig. 3. Double-skinned membrane surrounded by the Ru-based structured catalyst.

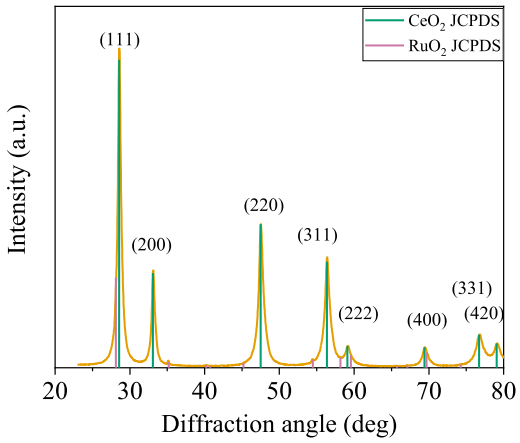

Fig. 4. XRD patterns of as-prepared 3 wt% Ru/CeO_2 catalyst.

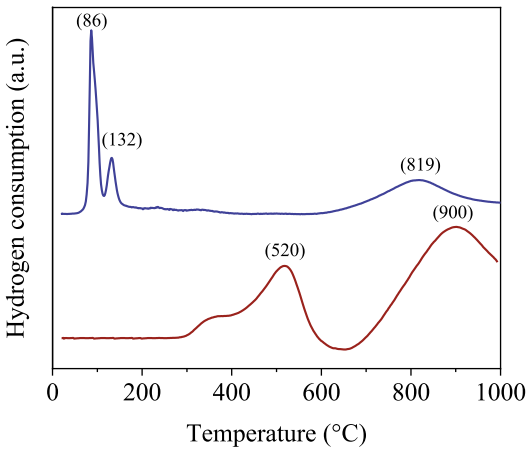

Fig. 5. H_2-TPR profiles of prepared 3 wt% Ru/CeO_2 catalyst and the CeO_2 support.

interactions enhance the Ru–CeO_2 interface, facilitating electron transfer during catalysis. These unique characteristics significantly enhance both the catalytic activity and thermal stability of the catalyst [40]. More specifically, Cha et al. investigated the relationship between catalyst structure and catalytic activity. The authors found out that metal-support interaction plays a crucial role in improving the catalytic activity for ammonia decomposition [41]. Crystallite size was determined employing Scherrer equation, based on the reflection observed for CeO_2 (111) crystallographic plane, yielding a value of approximately 12.5 nm. The results are aligned with findings from previous studies, which reported that smaller crystallite sizes lead to better dispersion, thereby enhancing catalytic performance [42]. This enhanced dispersion increases the availability of active sites, leading to superior catalytic performance.

The hydrogen reduction behavior of the produced samples, was investigated using H_2-TPR, and the findings are presented in Fig. 5. The H_2-TPR profile of the bare CeO_2 support was also provided for comparison purposes. This profile displays two distinct reduction regions: the low-temperature region (300–600 °C, with maximum at 520 °C) is associated to the reduction of surface oxygen while the high-temperature region (600–1000 °C, with maximum at 900 °C) is attributed to the reduction of bulk oxygen [43]. The presence of ruthenium induced significant modifications in the reduction profile of CeO_2, especially in the low-temperature zone. Indeed, the H_2-TPR pattern of Ru/CeO_2 catalyst is divided into three temperature regions. Low-temperature region (20–200 °C) shows a double peak, suggesting the presence of different ruthenium species interacting with the substrate with varying degrees of strength. Thus, the reduction peak at 86 °C could be assigned to the adsorbed oxygen or well dispersed ruthenium interacting strongly with CeO_2 surface [44], whereas the reduction peak at 132 °C could be attributed to the reduction of RuO_x particles that weakly interacted with CeO_2 surface [45]. A very low contribution is observed into the intermediate-temperature region (200–500 °C), due to CeO_2 surface oxygen reduction. Finally, the peak in the high temperature region (500–1000 °C) with maximum at 819 °C is ascribed to CeO_2 bulk oxygen reduction. Compared to bare CeO_2, these contributions are shifted to lower temperature due to interactions between RuO_x and support [46]. The catalyst's reducibility and its hydrogen consumption were further examined. The calculated hydrogen consumption was 15.6 $mmol_{H2}\ g^{-1}_{RuO2}$, leading to a reduction of 92.5 %.

In this study, the excellent dispersion is further confirmed by TEM images. Fig. 6 shows the TEM images of the synthesized structured catalyst. The acquired images displayed agglomerated catalyst particles with a primarily uniform circular morphology, varying in size from 30 to 127 nm (Fig. 6a). Agglomerates consisting of closely interlinked nanometric particles (~3–5 nm). Ruthenium clusters were not distinguishable on any of the samples, even in the magnified TEM images (Fig. 6b). This is likely due to the small particle size of ruthenium, which is highly dispersed on the Ce-based support, as well as the formation of a Ru–*O*–Ce solid solution, consistent with both XRD and TPR results. The particle size has a significant effect on catalytic activity. As reported by Karim et al., ammonia decomposition on Ru is highly structure-sensitive, with turnover frequency (TOF) varying significantly with the particle size growth [47]. Therefore, small ruthenium clusters seem particularly beneficial. More in detail, the magnification in Fig. 6c reports fringes with

d-spacing of 0.21 and 0.31 nm, attributed to the (101) and (111) planes of ruthenium and cerium oxide, respectively.

The SEM images of the bare OCF are presented in Fig. 7. The micrographs in Fig. 7 (a, b) display an appropriately rough surface, thus confirming that no additional steps are required to apply the catalytic layer. The peculiar morphology observed, featuring multiple anchorage points, enables the catalytic layer to strongly adhere to the substrate.

The analysis presented in Fig. 8a further demonstrates a uniform and well-distributed morphology of the catalytic layer, highlighting its consistent structural characteristics and homogeneity. Despite the relatively high catalyst loading (0.31 g cm^{-3}), the structured catalyst exhibits no signs of pores blockages phenomena. Hence, it can be concluded that the systematic and carefully controlled deposition of the

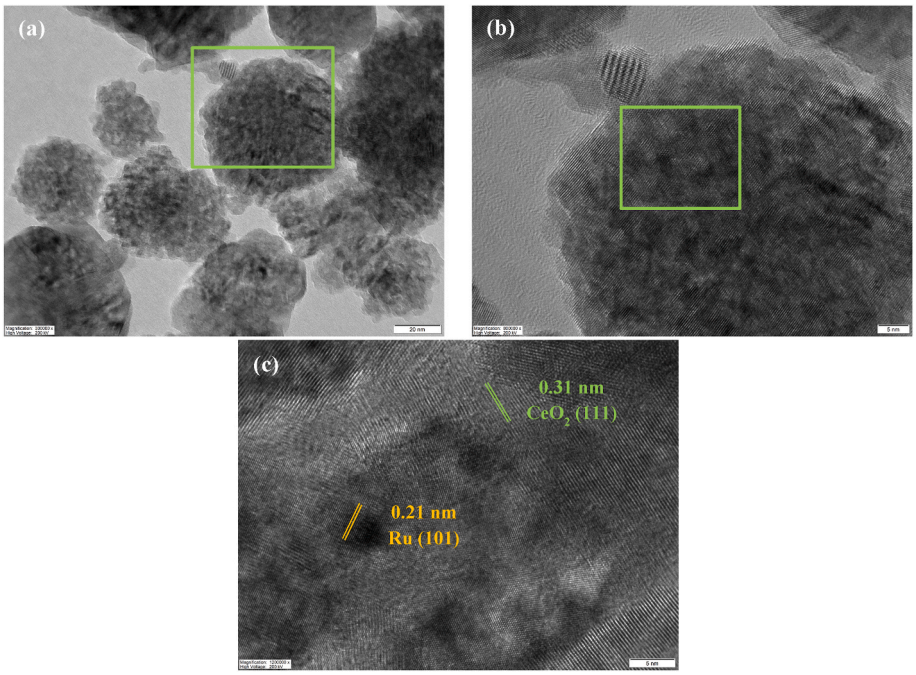

Fig. 6. TEM micrographs of 3 wt %Ru/CeO2 catalytic layer scraped from fresh OCF sample.

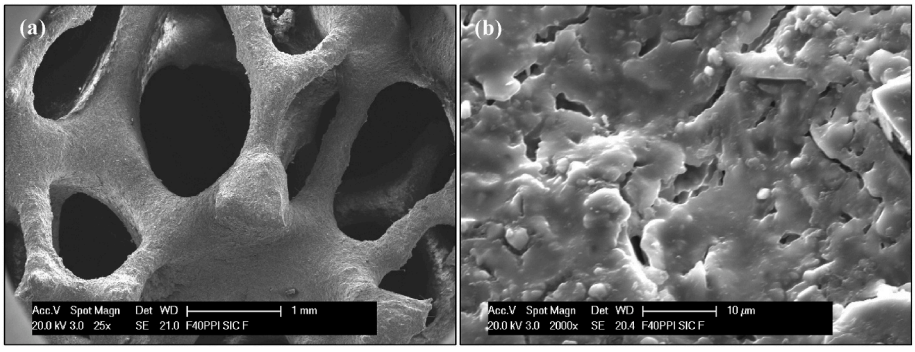

Fig. 7. SEM micrographs: (a) bare 40 PPI SiC OCF and (b) detail of the bare SiC OCF surface.

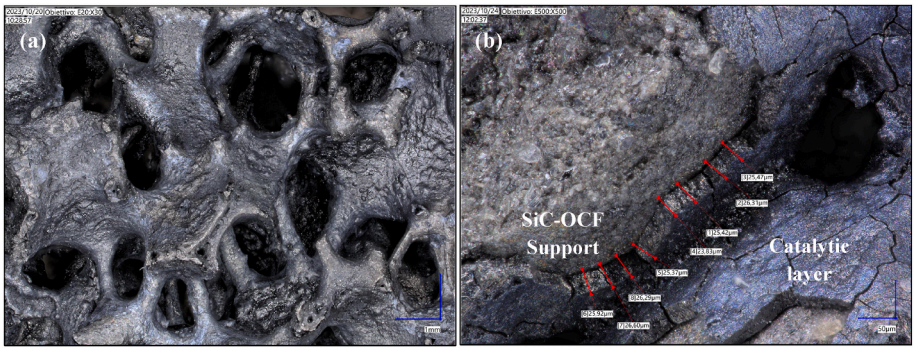

Fig. 8. Optical microscope images: (a) view of the catalytic layer deposited on SiC OCF; (b) cross-section view of catalytic layer thickness.

catalytic layer during the combustion process plays a critical role in ensuring uniform distribution, effectively preventing localized accumulation and minimizing the risk of structural defects. As a result, a precise control of the overall coating process is ensured, also when dealing with complex 3D structures. Furthermore, as illustrated in Fig. 8b, cross-sectional views obtained by intentionally fracturing a small section (strut) of the structured catalyst reveal a strong and well-integrated bond between the support and the coated layer. The thickness of the catalytic layer is observed to range between 23.83 and 26.60 µm, indicating uniform deposition and adherence.

Mechanical tests were carried out to assess the adhesion strength of the deposited layer. It is rather common to observe the detachement of catalytic layer from the substrate. The resulting weight loss (1.7 wt%) is in line with our previous works [37]. The mechanical stability was

linked to the uneven morphology of the support surface, which help the in situ crowing of the catalytic layer. This findings confirm the importance of this parameter, as it strongly influeces the adherence of catalytic layer to the carrier surface.

3.2. Structured membrane reactor performance evaluation

The performance of the structured membrane reactor within ammonia decomposition reaction was studied varying reaction temperature, reaction pressure and ammonia inlet flowrate. The relevant parameters evaluated include ammonia conversion, H_2 recovery and H_2 purity. With the purpose of highlighting the specifc advantages of the addition of a Pd-based membrane for hydrogen separation in a structured reactor. Ammonia conversion was first measured over the structured catalyst with the permeate side closed, thereby simulating the operation of a structured reactor. The achieved results have been used as reference. Then, to study the performace of the structured membrane reactor, the permeate line was opened, allowing the gases to flow through the membrane. Fig. 9 displays the evolution of the SMR performance as a function of the reaction temperature at fixed pressure (4 bar) and fixed flow rate (62 ml min^{-1}).

The integration of the Ru-based structured catalyst with the Pd-based membrane increased the ammonia conversion at lower temperatures, as it is depicted in Fig. 9a. This figure shows that more than 90 % of conversion can be reached already at 425 °C, suggesting that high conversion per pass is attainable. As expected, given the endothermicity of the reaction and the low decomposition rate, ammonia conversion is significanty limited at lower temperatures for both structured reactor (SR) and structured membrane reactor. However, it increases sharply as the temperature rises, as also reported in previous studies [48]. Furthermore, at fixed flow rate, the SMR is able to obtain similar ammonia conversion at reaction temperatures ~ 55 °C lower than the SR system. It is worth noting that the equilibrium conversion was approached in the SMR already at 425 °C. In agreement with other literature studies [49,50], the results highlight the benefits of the SMR technology, such as an ammonia conversion up to 29 % higher then the SR. Furthermore, the SMR reached 98.4 % conversion at 450 °C, with a corresponding hydrogen purity of 99.2 %. This improvements in industrial-scale applications have significant economic and practical benefits. It leads to higher production efficiency, as more hydrogen is produced with high purity. This translates to cost savings on reduced energy consumption, lowering overall operational costs. Additionally, the improved conversion results in higher yield per unit of reactant. Moreover, the in-situ removal of the product enhances overall efficiency since it minimizes the number of units as compared to sequential processes. Shared use of resources further optimizes the process, similarly to what observed in other systems [51].

Fig. 10a shows the effect of the operating pressure on the performance of both SR and SMR configurations. Ammonia conversion in the SMR increases along with the operating pressure, whereas in the SR increasing the pressure has a detrimental effect. Furthermore, Fig. 10b shows that operating pressure affects H_2 recovery, as increasing pressure, the driving force for permeation increases parallely, and this, in turn, enhances recovery. Moreover, the hydrogen permeation through the membrane decreases the concentration of hydrogen on the retentate side, thus subtracting a reaction product and, parallelly, shifting the equilibrium, according with the Le Châtelier's principle. The results presented are in line with previous studies, that report a higher ammonia conversion in membrane reactor sytstems compared to conventional systems [52]. Notably, according to the Temkin-Pyzhev rate mechanism, hydrogen has a detrimental effect on the ammonia decomposition reaction kinetic. This effect was previously reported for ruthenium-, iron- and platinum-based ammonia decomposition catalysts. As a result, the enhanced ammonia conversion can also be linked to a kinetic effect due to hydrogen extraction from the reaction environment [53,54]. Even though the increased pressure can be connected to a detrimental effect on the equilibrium, yet at 4 and 5.5 bar the SMR overcomes the equilibrium limits.

On the other hand, the increase of pressure results in a negative effect on the hydrogen purity in the permeate. This can be linked to the permeation mechanism of nitrogen and hydrogen through the membrane. Increasing the pressure leads to a higher nitrogen partial pressure in the reactor. As nitrogen permeation increases linearly with the nitrogen partial pressure, whereas hydrogen permeation increases with the square root of the pressure difference, a pressure increase consequently has a higher impact on nitrogen flux rather than on hydrogen flux. Thus, increasing the operating pressure reduces the purity of hydrogen separated by the membrane, but results in a higher recovery.

Fig. 11 shows the ammonia conversion as a function of the reaction temperature for the SMR in all the range of pressure tested.

As previously discussed with respect to Fig. 9, ammonia conversion in the SMR increases along with the operating temperature, in all the range of pressures tested. However, in a membrane reactor for ammonia decomposition the pressure increase has two main opposite effects. On one hand, ammonia conversion is positively influenced by pressure, as it provides an additional driving force for hydrogen permeation, removing one of the products and shifting the equilibrium according to the Le Châtelier's principle. On the contrary, ammonia conversion is negatively influenced by pressure because the ammonia decomposition reaction, which proceeds with a volume increase, is thermodinamically favoured at low pressures. The presence of this two opposite effects can explain why the higher conversion was achived at 4 bar at 380 °C.

The effect of the ammonia feed flow rate on ammonia conversion, H_2 purity and H_2 recovery for both systems operated at 480 °C and 4 bar is

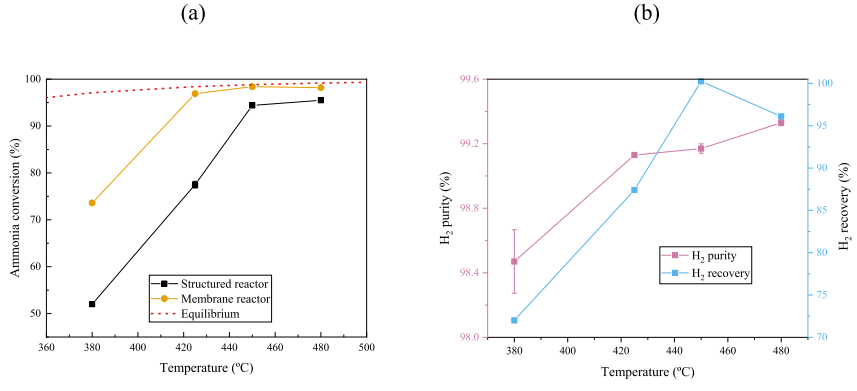

Fig. 9. (a) Ammonia conversion and (b) hydrogen purity and recovery as a function of the rection temperature at fixed pressure (4 bar) and feed flow rate (62 ml min^{-1}).

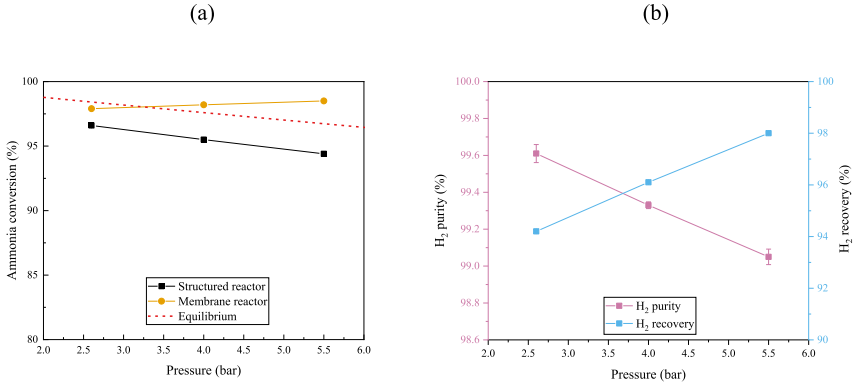

Fig. 10. (a) Ammonia conversion and (b) hydrogen purity and recovery as a function of the rection pressure at fixed temperature (480 °C) and feed flow rate (62 ml min^{-1}).

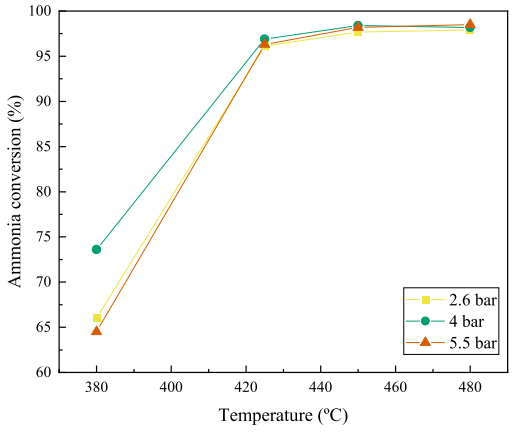

Fig. 11. Ammonia conversion in the SMR as a function of the rection temperature at different pressures and at fixed feed flow rate (62 ml min^{-1}).

reported in Fig. 12.

Specifically, for both SR and SMR configurations, ammonia conversion decreases as the ammonia feed flow rate increases. Parallelly, the obtained results show a lower H_2 recovery, due to the lower residence time, which corresponds to a higher hydrogen purity, reaching up to 99.8 %.

To the best of our knowledge, this work is the first study combining a structured catalyst and a palladium-based membrane for ammonia decomposition. The SiC-based OCF employed as carrier for the catalytic layer exhibits high thermostability, thermal conductivity, mechanical strength, and chemical inertness. The ability of this material to maintain a homogeneous temperature distribution within the catalyst for the ammonia decomposition reaction was also confirmed in previous literature [55]. Therefore, this study successfully integrates the properties of the fabricated structured catalyst with the developed membrane. The structured catalyst formulation proposed in this work offers a high surface area and active sites for ammonia decomposition, producing hydrogen at a rate that matches the high permeation capacity of the Pd-based membrane, possible due to the efficient solution-diffusion permeation mechanism. Additionally, the physical design of the catalyst and membrane system was optimized to minimize mass transfer limitations and ensure uniform hydrogen flow to the membrane. The membrane and catalyst must work synergistically to enable hydrogen produced from ammonia decomposition to permeate effectively through the membrane. To achieve coordination, the hydrogen permeation rate must match or exceed the production rate. This balance can be ensured by reducing the catalyst volume to limit hydrogen production if the membrane is a bottleneck or by increasing the membrane area to enhance permeation. Palladium-based membranes, with their high hydrogen permeability, facilitate this balance, avoiding limitations and optimizing system performance for ammonia decomposition and hydrogen extraction, however they operate within a specific temperature range of 400–550 °C [56]. This necessitates the use of catalysts that are active within this temperature range. The combination of the catalyst and membrane examined in this work meets these requirements, ensuring a matching of the working functions of both components. The beneficial effect of the structured catalyst for ammonia conversion

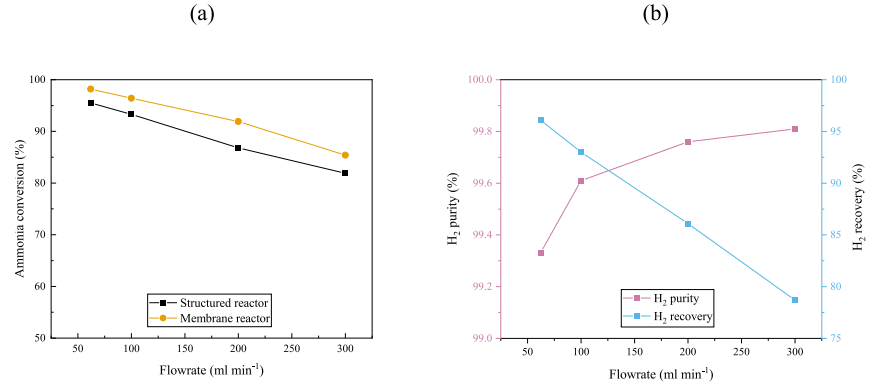

Fig. 12. (a) Ammonia conversion and (b) hydrogen purity and recovery as a function of the feed flow rate at fixed temperature (480 °C) and pressure (4 bar).

might be connected to the endothermicity of the reaction. Efficient radial heat transport and high radial mixing, ensured by the structured catalyst, play a crucial role in enhancing hydrogen production [57,58]. Furthermore, the large ratio between the geometric reaction surface area and the reaction volume, along with improved heat transfer rate per unit volume, contributed to the improved performance of the SMR reported in this work. Owing to the enhanced heat and mass transfer, the structured catalysts can represent a valid substitute of ceramic pellet catalysts in ammonia decomposition, ensuring an efficient and compact reactor design [59].

From an environmental standpoint, the proposed SMR for ammonia decomposition offers significant benefits over conventional systems. By integrating catalytic decomposition with hydrogen separation in a single unit, SMRs reduce carbon emissions and minimize the number of units, while enabling higher conversion efficiencies at lower temperatures. The reduced capital investment in auxiliary equipment and the smaller equipment footprint also lower operational and expansion costs, making the technology more scalable, sustainable and cost-effective [60,61].

4. Conclusions

A Ru-based structured catalyst has been successfully produced depositing a 3 wt% Ru/CeO_2 catalytic layer via In Situ-Solution Combustion Deposition method on a commercial 40 PPI SiC-based open-cell foam. The resulting thin and uniform catalytic layer showed an exeptional adhesion strength, as indicated by a weight loss of 1.7 wt%. The OFC-based catalyst was tested for ammonia decomposition reaction, in a structured membrane reactor. The catalyst, with ruthenium embedded in a CeO_2 matrix, exhibits strong metal-support interactions that enhance the Ru–CeO_2 interface. These interactions facilitate electron transfer during catalysis, significantly improving both catalytic activity and thermal stability. Results showed that the addition of the Pd-based membrane to the system leads to an increase in conversion up to 29 % compared with the catalyst alone in the structured reactor configuration. Furthermore, fixing the ammonia flow rate, the structured membrane reactor enabled similar conversion at operating temperatures approximately 55 °C lower than those of the conventional structured reactor. Moreover, the operating pressure was proved to significantly influence reactor performance; specifically, the structured membrane reactor was able ot overcome the equilibrium limitations at 4 and 5.5 bar at fixed temperature (480 °C) and feed flow rate (62 ml min^{-1}). The advantageous effects of the structured catalyst for ammonia conversion may be linked to the efficient radial heat transport and high radial mixing, that are crucial in enhancing hydrogen production. The structured design improves transport phenomena, ensuring uniform reactant flow and minimal thermal gradients. Integrated with a membrane for in situ H_2 separation, it shifts the equilibrium toward more ammonia decomposition. This combined reaction–separation approach enhances efficiency, lowers energy use, simplifies purification, and supports compact reactor configurations. These results open up a new route for ammonia decomposition in more compact and volumetrically efficent reactors.

CRediT authorship contribution statement

Jon Zuniga: Investigation, Conceptualization. **Gaetano Anello:** Writing – original draft, Methodology, Conceptualization. **Jorge J. Aragón:** Investigation, Formal analysis, Conceptualization. **María del Mar Díaz de Guereñu:** Methodology, Investigation. **Alba Arratibel:** Investigation. **Gabriel Marino:** Investigation. **Cristina Italiano:** Investigation. **Antonio Vita:** Writing – review & editing, Supervision, Investigation. **Fausto Gallucci:** Writing – review & editing, Supervision, Resources, Conceptualization.

Declaration of competing interest

The authors declare that they have no known competing financial interests or personal relationships that could have appeared to influence the work reported in this paper.

References

[1] Kovač A, Paranos M, Marciuš D. Hydrogen in energy transition: a review. Int J Hydrogen Energy 2021;46:10016–35. https://doi.org/10.1016/j.ijhydene.2020.11.256.

[2] Edwards PP, Kuznetsov VL, David WIF, Brandon NP. Hydrogen and fuel cells: towards a sustainable energy future. Energy Policy 2008;36:4356–62. https://doi.org/10.1016/J.ENPOL.2008.09.036.

[3] Capurso T, Stefanizzi M, Torresi M, Camporeale SM. Perspective of the role of hydrogen in the 21st century energy transition. Energy Convers Manag 2022;251:114898. https://doi.org/10.1016/j.enconman.2021.114898.

[4] Wan Z, Tao Y, Shao J, Zhang Y, You H. Ammonia as an effective hydrogen carrier and a clean fuel for solid oxide fuel cells. Energy Convers Manag 2021;228:113729. https://doi.org/10.1016/j.enconman.2020.113729.

[5] Yin SF, Xu BQ, Zhou XP, Au CT. A mini-review on ammonia decomposition catalysts for on-site generation of hydrogen for fuel cell applications. Appl Catal Gen 2004;277:1–9. https://doi.org/10.1016/j.apcata.2004.09.020.

[6] Su T, Guan B, Zhou J, Zheng C, Guo J, Chen J, Zhang Y, Yuan Y, Xie W, Zhou N, et al. Review on Ru-based and Ni-based catalysts for ammonia decomposition: research status, reaction mechanism, and perspectives. Energy Fuels 2023;37:8099–127. https://doi.org/10.1021/acs.energyfuels.3c00804.

[7] El-Shafie M, Kambara S, Hayakawa Y. Plasma-enhanced catalytic ammonia decomposition over ruthenium (Ru/Al2O3) and soda glass (SiO2) materials. J Energy Inst 2021;99:145–53. https://doi.org/10.1016/J.JOEI.2021.09.001.

[8] Andersen JA, Christensen JM, Østberg M, Bogaerts A, Jensen AD. Plasma-catalytic ammonia decomposition using a packed-bed dielectric barrier discharge reactor. Int J Hydrogen Energy 2022;47:32081–91. https://doi.org/10.1016/j.ijhydene.2022.07.102.

[9] Cechetto V, Anello G, Rahimalimamaghani A, Gallucci F. Carbon molecular sieve membrane reactors for ammonia cracking. Processes 2024;12:1168. https://doi.org/10.3390/pr12061168.

[10] Cechetto V, Di L, Gutierrez R. ScienceDirect ultra-pure hydrogen production via ammonia decomposition in a catalytic membrane reactor. Int J Hydrogen Energy 2022;47:21220–30. https://doi.org/10.1016/j.ijhydene.2022.04.240.

[11] Ho PH, Sanghez De Luna G, Ospitali F, Fornasari G, Vaccari A, Benito P. Open-cell foams coated by Ni/X/Al hydrotalcite-type derived catalysts (X = Ce, La, Y) for CO2methanation. J CO2 Util 2020;42. https://doi.org/10.1016/j.jcou.2020.101327.

[12] Baharudin L, Indera L AA, Watson MJ, Yip ACK. Process intensification in multifunctional reactors: a review of multi-functionality by catalytic structures, internals, operating modes, and unit integrations. Chemical Engineering and Processing - Process Intensification 2021;168:108561. https://doi.org/10.1016/J.CEP.2021.108561.

[13] Kapteijn F, Moulijn JA. Structured catalysts and reactors – perspectives for demanding applications. Catal Today 2022;383:5–14. https://doi.org/10.1016/J.CATTOD.2020.09.026.

[14] Xu X, Zhang S, Wang Y, Wang N, Jiang Q, Liu X, Guan Q, Zhang W. 2D surfaces twisted to enhance electron freedom toward efficient advanced oxidation processes. Appl Catal B Environ Energy 2024;345:123701. https://doi.org/10.1016/J.APCATB.2024.123701.

[15] Bracconi M, Ambrosetti M, Maestri M, Groppi G, Tronconi E. A fundamental analysis of the influence of the geometrical properties on the effective thermal conductivity of open-cell foams. Chemical Engineering and Processing - Process Intensification 2018;129:181–9. https://doi.org/10.1016/j.cep.2018.04.018.

[16] Tronconi E, Groppi G, Visconti CG. Structured catalysts for non-adiabatic applications. Curr Opin Chem Eng 2014;5:55–67. https://doi.org/10.1016/j.coche.2014.04.003.

[17] Aguirre A, Chandra V, Peters EAJF, Kuipers JAM, Neira D'Angelo MF. Open-cell foams as catalysts support: a systematic analysis of the mass transfer limitations. Chem Eng J 2020;393:124656. https://doi.org/10.1016/J.CEJ.2020.124656.

[18] Frey M, Bengaouer A, Geffraye G, Edouard D, Roger AC. Aluminum open cell foams as efficient supports for carbon dioxide methanation catalysts: pilot-scale reaction results. Energy Technol 2017;5:2078–85. https://doi.org/10.1002/ente.201700188.

[19] Bianchi E, Heidig T, Visconti CG, Groppi G, Freund H, Tronconi E. Heat transfer properties of metal foam supports for structured catalysts: wall heat transfer coefficient. Catal Today 2013;216:121–34. https://doi.org/10.1016/j.cattod.2013.06.019.

[20] Bracconi M, Ambrosetti M, Maestri M, Groppi G, Tronconi EA. Fundamental investigation of gas/solid mass transfer in open-cell foams using a combined experimental and CFD approach. Chem Eng J 2018;352:558–71. https://doi.org/10.1016/j.cej.2018.07.023.

[21] Moncada Quintero CW, Ercolino G, Poozhikunnath A, Maric R, Specchia S. Analysis of heat and mass transfer limitations for the combustion of methane emissions on PdO/Co3O4 coated on ceramic open cell foams. Chem Eng J 2021;405:126970. https://doi.org/10.1016/j.cej.2020.126970.

[22] Arratibel Plazaola A, Pacheco Tanaka DA, Van Sint Annaland M, Gallucci F. Recent advances in Pd-based membranes for membrane reactors. Molecules 2017;22:1–53. https://doi.org/10.3390/molecules22010051.

[23] Basile A, Gallucci F, Tosti S. Synthesis, characterization, and applications of palladium membranes. Membr Sci Technol 2008;13:255–323. https://doi.org/10.1016/S0927-5193(07)13008-4.

[24] Yun S, Ted Oyama S. Correlations in palladium membranes for hydrogen separation: a review. J Memb Sci 2011;375:28–45. https://doi.org/10.1016/j.memsci.2011.03.057.

[25] Israni SH, Nair BKR, Harold MP. Hydrogen generation and purification in a composite Pd hollow fiber membrane reactor: experiments and modeling. Catal Today 2009;139:299–311. https://doi.org/10.1016/j.cattod.2008.02.020.

[26] Nailwal BC, Chotalia P, Salvi J, Goswami N, Muhmood L, Adak AK, Kar S. Ammonia decomposition for hydrogen production using packed bed catalytic membrane reactor. Int J Hydrogen Energy 2024;49:1272–87. https://doi.org/10.1016/j.ijhydene.2023.09.229.

[27] Liu Y, Yin F, Li G, Tan Y. Preparation of silicon carbide supported iron catalysts and their catalytic activities in hydrogen production by ammonia decomposition. Catal Letters 2025;155. https://doi.org/10.1007/s10562-024-04858-w.

[28] Li Q, Yang Y, Wen Y, Zhang G, Xing W. Active gate driver with the independent suppression of overshoot and oscillation for SiC MOSFET modules. IEEE Trans Ind Electron 2024:1–11. https://doi.org/10.1109/tie.2024.3433436.

[29] Ricca A, Truda L, Palma V. Study of the role of chemical support and structured carrier on the CO2 methanation reaction. Chem Eng J 2019;377:120461. https://doi.org/10.1016/j.cej.2018.11.159.

[30] Moncada Quintero CW, Ercolino G, Poozhikunnath A, Maric R, Specchia S. Analysis of heat and mass transfer limitations for the combustion of methane emissions on PdO/Co3O4 coated on ceramic open cell foams. Chem Eng J 2021;405:126970. https://doi.org/10.1016/j.cej.2020.126970.

[31] Shao R, Zhang L, Wang L, Wang J, Zhang X, Han S, Cheng X, Wang Z. Cerium oxide-based catalyst for low-temperature and efficient ammonia decomposition for hydrogen production research. Int J Hydrogen Energy 2024;68:311–20. https://doi.org/10.1016/j.ijhydene.2024.04.197.

[32] Italiano C, Drago Ferrante G, Pino L, Laganà M, Ferraro M, Antonucci V, Vita A. Silicon carbide and alumina open-cell foams activated by Ni/CeO2-ZrO2 catalyst for CO2 methanation in a heat-exchanger reactor. Chem Eng J 2022;434. https://doi.org/10.1016/j.cej.2022.134685.

[33] Liu L, Yao Z, Deng Y, Gao F, Liu B, Dong L. Morphology and crystal-plane effects of nanoscale ceria on the activity of CuO/CeO2 for NO reduction by CO. ChemCatChem 2011;3:978–89. https://doi.org/10.1002/cctc.201000320.

[34] Gil S, Garcia-Vargas JM, Liotta LF, Pantaleo G, Ousmane M, Retailleau L, Giroir-Fendler A. Catalytic oxidation of propene over Pd catalysts supported on CeO2, TiO2, Al2O3and M/Al2O3oxides (M = Ce, Ti, Fe, Mn). Catalysts 2015;5:671–89. https://doi.org/10.3390/catal5020671.

[35] Italiano C, Llorca J, Pino L, Ferraro M, Antonucci V, Vita A. CO and CO2 methanation over Ni catalysts supported on CeO2, Al2O3 and Y2O3 oxides. Appl Catal, B 2020;264:118494. https://doi.org/10.1016/j.apcatb.2019.118494.

[36] Chen L, Zhou W, Huo C, Li L, Cui M, Qiao X, Fei Z. Improved metal-support interaction in Ru/CeO2 catalyst via plasma-treated strategy for dichloroethane oxidation. Appl Catal Gen 2023;660:119215. https://doi.org/10.1016/j.apcata.2023.119215.

[37] Italiano C, Drago Ferrante G, Pino L, Laganà M, Ferraro M, Antonucci V, Vita A. Silicon carbide and alumina open-cell foams activated by Ni/CeO2-ZrO2 catalyst for CO2 methanation in a heat-exchanger reactor. Chem Eng J 2022;434. https://doi.org/10.1016/j.cej.2022.134685.

[38] Arratibel A, Pacheco Tanaka A, Laso I, van Sint Annaland M, Gallucci F. Development of Pd-based double-skinned membranes for hydrogen production in fluidized bed membrane reactors. J Memb Sci 2018;550:536–44. https://doi.org/10.1016/j.memsci.2017.10.064.

[39] Liu P, Niu R, Li W, Wang S, Li J. Morphology effect of ceria on the ammonia synthesis activity of Ru/CeO 2 catalysts. Catal Letters 2019;149:1007–16. https://doi.org/10.1007/s10562-019-02674-1.

[40] Liu H, Zhang Y, Liu S, Li S, Liu G. Ni-CeO2 nanocomposite with enhanced metal-support interaction for effective ammonia decomposition to hydrogen. Chem Eng J 2023;473:145371. https://doi.org/10.1016/J.CEJ.2023.145371.

[41] Cha J, Lee T, Lee YJ, Jeong H, Jo YS, Kim Y, Nam SW, Han J, Lee KB, Yoon CW, et al. Highly monodisperse sub-nanometer and nanometer Ru particles confined in alkali-exchanged zeolite Y for ammonia decomposition. Appl Catal, B 2021;283:119627. https://doi.org/10.1016/J.APCATB.2020.119627.

[42] Chen C, Fan X, Zhou C, Lin L, Luo Y, Au C, Cai G, Wang X, Jiang L. Hydrogen production from ammonia decomposition over Ni/CeO2 catalyst: effect of CeO2 morphology. J Rare Earths 2023;41:1014–21. https://doi.org/10.1016/J.JRE.2022.05.001.

[43] Pino L, Vita A, Cipitì F, Laganà M, Recupero V. Hydrogen production by methane tri-reforming process over Ni–ceria catalysts: effect of La-doping. Appl Catal, B 2011;104:64–73. https://doi.org/10.1016/J.APCATB.2011.02.027.

[44] Lin B, Liu Y, Heng L, Wang X, Ni J, Lin J, Jiang L. Morphology effect of ceria on the catalytic performances of Ru/CeO2 catalysts for ammonia synthesis. Ind Eng Chem Res 2018;57:9127–35. https://doi.org/10.1021/acs.iecr.8b02126.

[45] Gil S, Garcia-Vargas JM, Liotta LF, Pantaleo G, Ousmane M, Retailleau L, Giroir-Fendler A. Catalytic oxidation of propene over Pd catalysts supported on CeO2, TiO2, Al2O3and M/Al2O3oxides (M = Ce, Ti, Fe, Mn). Catalysts 2015;5:671–89. https://doi.org/10.3390/catal5020671.

[46] Vita A, Italiano C, Pino L, Laganà M, Recupero V. Hydrogen-rich gas production by steam reforming of n-dodecane. Part II: stability, regenerability and sulfur poisoning of low loading Rh-based catalyst. Appl Catal, B 2017;218:317–26. https://doi.org/10.1016/j.apcatb.2017.06.059.

[47] Karim AM, Prasad V, Mpourmpakis G, Lonergan WW, Frenkel AI, Chen JG, Vlachos DG. Correlating particle size and shape of supported Ru/γ-Al 2O3 catalysts with NH3 decomposition activity. J Am Chem Soc 2009;131:12230–9. https://doi.org/10.1021/ja902587k.

[48] Itoh N, Oshima A, Suga E, Sato T. Kinetic enhancement of ammonia decomposition as a chemical hydrogen carrier in palladium membrane reactor. Catal Today 2014;236:70–6.

[49] García-García FR, Ma YH, Rodríguez-Ramos I, Guerrero-Ruiz A. High purity hydrogen production by low temperature catalytic ammonia decomposition in a multifunctional membrane reactor. Catal Commun 2008;9:482–6. https://doi.org/10.1016/j.catcom.2007.07.036.

[50] Lee JE, Lee J, Jeong H, Park YK, Kim BS. Catalytic ammonia decomposition to produce hydrogen: a mini-review. Chem Eng J 2023;475:146108. https://doi.org/10.1016/j.cej.2023.146108.

[51] Hua Z, Song H, Zhou C, Xin Q, Zhou F, Fan W, Liu S, Zhang X, Zheng C, Yang Y, et al. A promising catalyst for catalytic oxidation of chlorobenzene and slipped ammonia in SCR exhaust gas: investigating the simultaneous removal mechanism. Chem Eng J 2023;473:145106. https://doi.org/10.1016/J.CEJ.2023.145106.

[52] Liu J, Ju X, Tang C, Liu L, Li H, Chen P. High performance stainless-steel supported Pd membranes with a finger-like and gap structure and its application in NH3 decomposition membrane reactor. Chem Eng J 2020;388:124245.

[53] Lamb K, Hla SS, Dolan M. Ammonia decomposition kinetics over LiOH-promoted, A-Al2O3-supported Ru catalyst. Int J Hydrogen Energy 2019;44:3726–36. https://doi.org/10.1016/j.ijhydene.2018.12.123.

[54] Di Carlo A, Vecchione L, Del Prete Z. Ammonia decomposition over commercial Ru/Al2O3 catalyst: an experimental evaluation at different operative pressures and temperatures. Int J Hydrogen Energy 2014;39:808–14. https://doi.org/10.1016/j.ijhydene.2013.10.110.

[55] Pinzón M, Romero A, de Lucas Consuegra A, de la Osa AR, Sánchez P. Hydrogen production by ammonia decomposition over ruthenium supported on SiC catalyst. J Ind Eng Chem 2021;94:326–35. https://doi.org/10.1016/j.jiec.2020.11.003.

[56] Cerrillo JL, Morlanés N, Kulkarni SR, Realpe N, Ramírez A, Katikaneni SP, Paglieri SN, Lee K, Harale A, Solami B, et al. High purity, self-sustained, pressurized hydrogen production from ammonia in a catalytic membrane reactor. Chem Eng J 2022;431. https://doi.org/10.1016/j.cej.2021.134310.

[57] Young K, Been H, Song D, Jung U. ScienceDirect ammonia decomposition over Ru-coated metal- structured catalysts for COx-free hydrogen production. Int J Hydrogen Energy 2023;52:534–45. https://doi.org/10.1016/j.ijhydene.2023.08.004.

[58] Sinn C, Wentrup J, Pesch GR, Thöming J, Kiewidt L. Chemical engineering research and design structure-heat transport analysis of periodic open-cell foams to Be used as catalyst carriers, vol. 6; 2020. p. 209–19. https://doi.org/10.1016/j.cherd.2020.12.007.

[59] Ho PH, Ambrosetti M, Groppi G, Tronconi E, Palkovits R, Fornasari G, Vaccari A, Benito P. Metallic foams for energy and environmental applications. first ed.vol 178. Elsevier B.V.; 2019. ISBN 9780444641274.

[60] Kim H, Gu J, Byun M, Choe C, Lim H. Novel propane dehydrogenation process design integrated with membrane reactor and solid oxide fuel cell: economic and environmental aspects. J Environ Chem Eng 2023;11:110830. https://doi.org/10.1016/J.JECE.2023.110830.

[61] Fang J, Jin X, Huang K. Life cycle analysis of a combined CO2 capture and conversion membrane reactor. J Memb Sci 2018;549:142–50. https://doi.org/10.1016/J.MEMSCI.2017.12.006.